Finite element for non-stationary problems of viscoelastic orthotropic beams

M. Zajíček[a,*], V. Adámek[a], J. Dupal[a]

[a]*Faculty of Applied Sciences, University of West Bohemia, Univerzitní 22, 306 14 Plzeň, Czech Republic*

Abstract

The main aim of this work is to derive a finite beam element especially for solving of non-stationary problems of thin viscoelastic orthotropic beams. Presented approach combines the Timoshenko beam theory with the consideration of nonzero axial strain. Furthermore, the discrete Kelvin-Voight material model was employed for the description of beam viscoelastic material behaviour. The presented finite beam element was derived by means of the principle of virtual work. The beam deflection and the slope of the beam have been determined by the analytical and numerical (FEM) approach. These studies were made in detail on the simple supported beam subjected to the non-stationary transverse continuous loading described by the cosine function in space and by the Heaviside function in time domain. The study shows that beam deformations obtained by using derived finite element give a very good agreement with the analytical results.

1. Introduction

This work concerns the solution of the planar problem of a thin straight orthotropic viscoelastic beam subjected to a non-stationary loading. The main aim of this study is to derive the finite beam element based on the approximate Timoshenko beam theory and to compare analytical and numerical results for a particular beam problem. The purpose of this effort is to use such element for the effective numerical solution of beam-like structures inverse problems with minimal loss of solution accuracy. It is well known fact that inverse problems, e.g. material parameters identification etc., are usually very time-consuming and so the demand for effective computation is one of the most important (see e.g. [7]).

Many authors were concerned with analytical as well as finite element solutions of beam problems. The classical Euler-Bernoulli beam theory [2, 4] is restricted for thin beams and does not include the effect of shear forces on the beam deformation. Due to this limitation, in 1921 Timoshenko developed a beam theory including the effect of the transverse shear deformation which is assumed constant across the thickness of the beam and depends on the shear correction factor (see e.g. [2, 4]). Further, Chandrashekhara et al. [6] employed the analytical solution for the free vibration of laminated composite beams including the transverse (first-order) shear deformation effects and the rotary inertia. The solution procedure is applicable to arbitrary boundary conditions. Two higher order displacement based on shear deformation theories of free vibration analysis of laminated composite beams is carried out for example in [8].

---

*Corresponding author. Tel.: +420 377 632 328, e-mail: zajicek@kme.zcu.cz.

Finite elements have also been developed based on the Timoshenko theory as could be found in [3,10] or [12]. Most of these finite element models possess a two node-two degree of freedom structure because the requirements of the variational principle for the Timoshenko's displacement field are accepted. Davis et al. showed in [3] that a Timoshenko beam element converged to the exact solution of the elasticity equations for a simply supported beam provided that the correct value of the shear factor is used. Thomas and Abbas [10] presented for the first time a finite element model with nodal degrees of freedom which can satisfy all the forced and the natural boundary conditions of a Timoshenko beam. The mass and stiffness matrices of the element are derived from kinetic and strain energies by assigning polynomial expressions for total deflection and bending slope. Zienkiewicz and Taylor [12] give a summary of finite element models for the Euler-Bernoulli and the Timoshenko theory. A mathematical framework from which general problems may be formulated and solved using variational and Galerkin methods is presented. In addition, these authors consider problem of shape functions for situations in which the approximating functions (displacement and slope) are necessary C^0 and C^1 continuous. Zienkiewicz and Taylor also cover in some detail formulations for viscoelasticity, plasticity and viscoplasticity material models.

One can find several types of already derived finite beam elements which employed a higher order shear deformation theories. A second-order beam theory requiring two coefficients, one for cross-sectional warping and the second for transverse direct stress, was developed by Stephen and Levinson [9]. Heyliger and Reddy [5] used a higher order beam finite element for bending and vibration problems. In this formulation, the theory assumes a cubic variation of the in-plane displacement in thickness co-ordinate and a parabolic variation of the transverse shear stress across the thickness of the beam. Further this theory satisfies the zero shear strain conditions at the top and bottom surfaces of the beam and neglects the effect of the transverse normal strain. Subramanian [8] furthermore carried out two-node C^1 finite elements of eight degrees of freedom per node for the vibration problems of the laminated composite beams. Applied theories not only include the effect of transverse shear strain and normal strain but also satisfy free transverse shear strain/stress conditions on the top and bottom lateral surfaces of the beams.

This paper relates to the work [11] in which the analytical solution of static and free vibration problem of a uniform and linear elastic beam has been derived. In addition, results obtained in [1], where authors presented analytical and numerical solution of non-stationary vibrations of a thin viscoelastic beam, were utilized. In both mentioned works, beams were supposed as orthotropic and thin and their formulations were based on the Timoshenko beam theory.

2. Problem formulation

We generally consider a straight beam of length $2l$ consisting of n layers which are perfectly bonded. Let us number these layers from the lower to the upper face as shown in Fig. 1. The overall thickness of the laminated beam is h. Homogenous, orthotropic and linear viscoelastic (Kelvin-Voight model) material properties of layers are supposed. Each layer k is referred to by the x_3 coordinates of its lower face h_{k-1} and upper face h_k. The angle θ_k is the orientation of the kth layer (in directions L, T, T') with respect to the x_1-axis. The cross-section area of beams can have various geometries (with the width b) but must be uniform along the x_1-axis and symmetric to the x_3-axis. Furthermore, the general combination of lateral and axial loading may be applied but only bending and stretching in the $x_1 - x_3$ plane of symmetry can exist. This is the reason why only displacements $u_1(x_1, x_3, t)$ and $u_3(x_1, t)$ in the x_1 and x_3 directions,
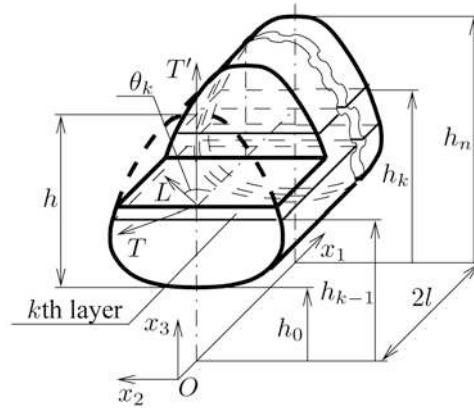
Fig. 1. A thin laminated beam with a symmetric cross-section

respectively, may be nonzero if the assumption is accepted that Poisson's effects may cause deformations only in the $x_1 - x_3$ plane.

The displacement fields for the first-order shear deformation theory are taken as

$$u_1(x_1, x_3, t) = u(x_1, t) + x_3\, \psi(x_1, t) \qquad \text{and} \qquad u_3(x_1, t) = w(x_1, t)\,, \tag{1}$$

where $u(x_1, t)$ is the displacement due to extension, $w(x_1, t)$ is the displacement due to bending and $\psi(x_1, t)$ represents rotation of the transverse normal referred to the plane $x_3 = 0$. Besides, $u(x_1, t)$ can be expressed in the form

$$u(x_1, t) = u_c(x_1, t) - z_c\psi(x_1, t) \tag{2}$$

with the help of displacement $u_c(x_1, t)$ in centroidal axis direction when the distance of this axis and x_1-axis is

$$z_c = \frac{B_{11}}{A_{11}}\,, \tag{3}$$

where B_{11} and A_{11} are stiffness parameters well-known in the laminate theory (see e.g. [11]). The nonzero strain-displacement relationships for presented theory are then given as

$$\varepsilon_{11}(x_1, x_3, t) = \frac{\partial u_1}{\partial x_1} = \frac{\partial u}{\partial x_1} + x_3 \frac{\partial \psi}{\partial x_1}\,, \quad 2\,\varepsilon_{31}(x_1, t) = \frac{\partial u_3}{\partial x_1} + \frac{\partial u_1}{\partial x_3} = \frac{\partial w}{\partial x_1} + \psi = \gamma(x_1, t)\,. \tag{4}$$

To make following relations more transparent, the notation for strain and stress tensor components are reduced to $\varepsilon_{11} = \varepsilon_1, 2\,\varepsilon_{31} = \varepsilon_5, \sigma_{11} = \sigma_1$ and $\sigma_{31} = \sigma_5$. The stress-strain relationships for the kth layer is then, with respect of (4), taken as

$$\sigma_i^k = Q_{ii}^k \varepsilon_i + \widetilde{Q}_{ii}^k \dot{\varepsilon}_i \qquad \text{for} \qquad i = 1, 5\,, \tag{5}$$

where

$$Q_{11}^k = \frac{E_1}{1 - \mu_{12}\mu_{21}}\,, \qquad Q_{55}^k = G_{31}\,, \qquad \widetilde{Q}_{11}^k = \frac{\lambda_1}{1 - \nu_{12}\nu_{21}} \qquad \text{and} \qquad \widetilde{Q}_{55}^k = \eta_{31} \tag{6}$$

are the reduced material constants. It is obvious that the Young's modulus E_1 is equal to the longitudinal modulus E_L and the transverse modulus E_T for $\theta_k = 0$ and $\theta_k = 90$, respectively. It is similarly valid for the coefficient of normal viscosity λ_1. The other material constants (i.e. the Poisson's ratios μ_{12}, μ_{21} and ν_{12}, ν_{21} of elastic and viscous elements in material model, respectively, shear modulus G_{31} and the coefficient of shear viscosity η_{31}) in coordinate system x_1, x_2, x_3 are the same as in the coordinate system L, T, T' for both angles θ_k.

3. Finite element formulation

In this paper, the shape functions are formulated using weak form for linear elastic rods, see [12]. When the longitudinal and centroidal axes are identical, the displacement field can be restricted to bending and axial strains, eqs. (1) and (2). Then the solution of rod problem involves finding one-dimensional interpolations to approximate each of these functions appearing in the weak form.

Zienkiewicz and Taylor bring in [12] that the weight function for the axial deformation and the static problem must satisfy the exact solution of the adjoint homogeneous ordinary differential equation of the second order. Therefore the linear polynomial

$$u_c(x_1, t) = [1, x_1][a_0(t), a_1(t)]^T = \boldsymbol{\phi}_1(x_1)\boldsymbol{c}_1(t) \tag{7}$$

is selected to describe the centroidal deformation. If a static behaviour of the Euler-Bernoulli beam is considered, the exact interpolation for the transverse displacement can be also found. In order to obtain exact interelement nodal solution for ordinary differential equation, the interpolation function for the weight function must satisfy the exact solution of the adjoint homogeneous differential equation of the fourth order as mentioned in [12]. It is the reason why a polynomial of cubic order for Euler-Bernoulli beam shape function is to use, i.e.

$$w(x_1, t) = \left[1, x_1, x_1^2, x_1^3\right][a_2(t), a_3(t), a_4(t), a_5(t)]^T = \boldsymbol{\phi}_2(x_1)\boldsymbol{c}_2(t) \,. \tag{8}$$

It could be also found in [12] that the proposed transverse and centroidal axis displacement approximations may be used in transient analysis as well, however then the solution is no longer be exact at the interelement nodes. Therefore vectors $\boldsymbol{c}_1(t)$ and $\boldsymbol{c}_2(t)$ in (7) and (8) are generally assumed time-dependent.

Implementation of the transverse shear strain contribution to the rotation angle about the coordinate axis x_2, i.e. the application of the Timoshenko theory, was made by the next way. We consider equations of motion

$$B_{11}u''(x_1) + D_{11}\psi''(x_1) - \alpha A_{55}\gamma(x_1) = 0 \,, \tag{9}$$

see [11], where inertial forces were neglected and distributed forces per length on the beam faces are omitted. It means in consequence that the transverse force and transverse shear strain are constant along the element length. Inserting displacement approximations mentioned above into modified balance equations, we are able to determine the rotation angle including the transverse shear strain

$$\psi(x_1, t) = \gamma - \frac{\partial w}{\partial x_1} = [\boldsymbol{\phi}_5 - \boldsymbol{\phi}_2'(x_1)]\,\boldsymbol{c}_2(t) = \boldsymbol{\phi}_3(x_1)\boldsymbol{c}_2(t) \tag{10}$$

with

$$\boldsymbol{\phi}_5 = [0, 0, 0, -6\,D_T/(\alpha A_{11}A_{55})] \qquad \text{and} \qquad D_T = A_{11}D_{11} - B_{11}^2 \,. \tag{11}$$

The parameter α is the shear correction factor and may be calculated as shown in [11]. The stiffness constants are defined as follows

$$(A_{11}, B_{11}, D_{11}) = \sum_{k=1}^{n} Q_{11}^k \int_{h_{k-1}}^{h_k} b(x_3)(1, x_3, x_3^2)\,\mathrm{d}x_3 \,, \qquad A_{55} = \sum_{k=1}^{n} Q_{55}^k \int_{h_{k-1}}^{h_k} b(x_3)\,\mathrm{d}x_3 \,. \tag{12}$$

Now we consider the division of the beam domain V into a set of disjoint subdomains V^e such that the sum over the element domains V^e is equal to V. Similarly the boundary is divided

into subdomains. Because the finite beam element is developed by means of the principle of virtual work (see e.g. [12]), we obtain after some simplifications the relation

$$\sum_e \left\{ \sum_{j=1,5} \int_{V^e} \delta\varepsilon_j \, \sigma_j \, \mathrm{d}V + \sum_{i=1,3} \left[\int_{V^e} \delta u_i \, (\rho \, \ddot{u}_i - X_i) \, \mathrm{d}V - \int_{A_p^e} \delta u_i \, p_i \, \mathrm{d}A \right] \right\} = 0 \,, \qquad (13)$$

where A_p^e is a boundary segment on which tractions p_i are specified and where X_i are body force components. It follows from (13) that the definition of the local axis x_e within the domain V^e of each element is useful. Consequently, generalized deformations in element nodes may be given as

$$\boldsymbol{q}_1(t) = [u(0,t), u(l_e,t)]^T \qquad \text{and} \qquad \boldsymbol{q}_2(t) = [w(0,t), w(l_e,t), \psi(0,t), \psi(l_e,t)]^T, \qquad (14)$$

while the finite element is considered of length l_e. Using the approximate functions (7), (8) and (10) which are expressed in local coordinates leads to the system of equations

$$\begin{bmatrix} \boldsymbol{q}_1(t) \\ \boldsymbol{q}_2(t) \end{bmatrix} = \begin{bmatrix} \boldsymbol{S}_{11} & -z_c\boldsymbol{S}_{12} \\ \boldsymbol{0} & \boldsymbol{S}_{22} \end{bmatrix} \begin{bmatrix} \boldsymbol{c}_1(t) \\ \boldsymbol{c}_2(t) \end{bmatrix}, \; \boldsymbol{S}_{11} = \begin{bmatrix} \phi_1(0) \\ \phi_1(l_e) \end{bmatrix}, \; \boldsymbol{S}_{12} = \begin{bmatrix} \phi_3(0) \\ \phi_3(l_e) \end{bmatrix}, \; \boldsymbol{S}_{22} = \begin{bmatrix} \phi_2(0) \\ \phi_2(l_e) \\ \phi_3(0) \\ \phi_3(l_e) \end{bmatrix}. \; (15)$$

Solving the equation (15), we get time-dependent functions

$$\boldsymbol{c}_1(t) = \boldsymbol{S}_{11}^{-1}\boldsymbol{q}_1(t) + z_c\boldsymbol{S}_{11}^{-1}\boldsymbol{S}_{12}\boldsymbol{S}_{22}^{-1}\boldsymbol{q}_2(t) \qquad \text{and} \qquad \boldsymbol{c}_2(t) = \boldsymbol{S}_{22}^{-1}\boldsymbol{q}_2(t) \,. \qquad (16)$$

Substituting this result into (7), (8) and (10), the finite element approximation for displacements could be rewritten as follows

$$\begin{aligned} u(x_e,t) &= \phi_1(x_e)\boldsymbol{S}_{11}^{-1}\boldsymbol{q}_1(t) + \phi_4(x_e)\boldsymbol{S}_{22}^{-1}\boldsymbol{q}_2(t) \,, \\ w(x_e,t) &= \phi_2(x_e)\boldsymbol{S}_{22}^{-1}\boldsymbol{q}_2(t) \,, \\ \psi(x_e,t) &= \phi_3(x_e)\boldsymbol{S}_{22}^{-1}\boldsymbol{q}_2(t) \end{aligned} \qquad (17)$$

with

$$\phi_4(x_e) = z_c \left[\phi_1(x_e)\boldsymbol{S}_{11}^{-1}\boldsymbol{S}_{12} - \phi_3(x_e) \right] \,. \qquad (18)$$

To derive mass, stiffness and damping matrices of the finite element using the principle of virtual work, eqs. (4), (5) and (17) are substituted into (13). If the matrix $\boldsymbol{I}_{ij}^{kl}$ is defined as

$$\boldsymbol{I}_{ij}^{kl} = \int_0^{l_e} \frac{\partial^i \boldsymbol{\phi}_k^T}{\partial x_e^i} \frac{\partial^j \boldsymbol{\phi}_l}{\partial x_e^j} \, \mathrm{d}x_e \,, \qquad (19)$$

we can write

$$\sum_{i=1,3} \int_{V^e} \rho \, \delta u_i \, \ddot{u}_i \, \mathrm{d}V = \left[\delta\boldsymbol{q}_1^T(t), \delta\boldsymbol{q}_2^T(t) \right] \begin{bmatrix} \boldsymbol{M}_{e11} & \boldsymbol{M}_{e12} \\ \boldsymbol{M}_{e12}^T & \boldsymbol{M}_{e22} \end{bmatrix} \begin{bmatrix} \ddot{\boldsymbol{q}}_1(t) \\ \ddot{\boldsymbol{q}}_2(t) \end{bmatrix} = \delta\boldsymbol{q}_e^T(t) \, \boldsymbol{M}_e \, \ddot{\boldsymbol{q}}_e(t) \,, \qquad (20)$$

$$\sum_{j=1,5} \int_{V^e} \delta\varepsilon_j \, \sigma_j \, \mathrm{d}V = \left[\delta\boldsymbol{q}_1^T(t), \delta\boldsymbol{q}_2^T(t) \right] \left\{ \begin{bmatrix} \boldsymbol{K}_{e11} & \boldsymbol{K}_{e12} \\ \boldsymbol{K}_{e12}^T & \boldsymbol{K}_{e22} \end{bmatrix} \begin{bmatrix} \boldsymbol{q}_1(t) \\ \boldsymbol{q}_2(t) \end{bmatrix} + \begin{bmatrix} \boldsymbol{B}_{e11} & \boldsymbol{B}_{e12} \\ \boldsymbol{B}_{e12}^T & \boldsymbol{B}_{e22} \end{bmatrix} \begin{bmatrix} \dot{\boldsymbol{q}}_1(t) \\ \dot{\boldsymbol{q}}_2(t) \end{bmatrix} \right\} =$$
$$\delta\boldsymbol{q}_e^T(t) \left\{ \boldsymbol{K}_e \, \boldsymbol{q}_e(t) + \boldsymbol{B}_e \, \dot{\boldsymbol{q}}_e(t) \right\} \,, \qquad (21)$$

where

$$
\begin{aligned}
\boldsymbol{M}_{e11} &= \boldsymbol{S}_{11}^{-T}\rho_{11}\boldsymbol{I}_{00}^{11}\boldsymbol{S}_{11}^{-1}, \\
\boldsymbol{M}_{e12} &= \boldsymbol{S}_{11}^{-T}\big[\rho_{11}\boldsymbol{I}_{00}^{14} + R_{11}\boldsymbol{I}_{00}^{13}\big]\boldsymbol{S}_{22}^{-1}, \\
\boldsymbol{M}_{e22} &= \boldsymbol{S}_{22}^{-T}\big[\rho_{11}\big(\boldsymbol{I}_{00}^{22} + \boldsymbol{I}_{00}^{44}\big) + R_{11}\big(\boldsymbol{I}_{00}^{34} + \boldsymbol{I}_{00}^{43}\big) + I_{11}\boldsymbol{I}_{00}^{33}\big]\boldsymbol{S}_{22}^{-1},
\end{aligned}
\tag{22}
$$

$$
\begin{aligned}
\boldsymbol{K}_{e11} &= \boldsymbol{S}_{11}^{-T}A_{11}\boldsymbol{I}_{11}^{11}\boldsymbol{S}_{11}^{-1}, \\
\boldsymbol{K}_{e12} &= \boldsymbol{S}_{11}^{-T}\big[A_{11}\boldsymbol{I}_{11}^{14} + B_{11}\boldsymbol{I}_{11}^{13}\big]\boldsymbol{S}_{22}^{-1}, \\
\boldsymbol{K}_{e22} &= \boldsymbol{S}_{22}^{-T}\big[A_{11}\boldsymbol{I}_{11}^{44} + \alpha A_{55}\boldsymbol{I}_{00}^{55} + B_{11}\big(\boldsymbol{I}_{11}^{34} + \boldsymbol{I}_{11}^{43}\big) + D_{11}\boldsymbol{I}_{11}^{33}\big]\boldsymbol{S}_{22}^{-1},
\end{aligned}
\tag{23}
$$

$$
\begin{aligned}
\boldsymbol{B}_{e11} &= \boldsymbol{S}_{11}^{-T}\widetilde{A}_{11}\boldsymbol{I}_{11}^{11}\boldsymbol{S}_{11}^{-1}, \\
\boldsymbol{B}_{e12} &= \boldsymbol{S}_{11}^{-T}\big[\widetilde{A}_{11}\boldsymbol{I}_{11}^{14} + \widetilde{B}_{11}\boldsymbol{I}_{11}^{13}\big]\boldsymbol{S}_{22}^{-1}, \\
\boldsymbol{B}_{e22} &= \boldsymbol{S}_{22}^{-T}\big[\widetilde{A}_{11}\boldsymbol{I}_{11}^{44} + \alpha\widetilde{A}_{55}\boldsymbol{I}_{00}^{55} + \widetilde{B}_{11}\big(\boldsymbol{I}_{11}^{34} + \boldsymbol{I}_{11}^{43}\big) + \widetilde{D}_{11}\boldsymbol{I}_{11}^{33}\big]\boldsymbol{S}_{22}^{-1}.
\end{aligned}
\tag{24}
$$

In these relations, we can find other parameters except A_{11}, B_{11}, D_{11} and A_{55} defined by (12). Then, the mass moment of inertia terms are given as

$$
(\rho_{11}, R_{11}, I_{11}) = \sum_{k=1}^{n}\rho^k\int_{h_{k-1}}^{h_k}b(x_3)(1, x_3, x_3^2)\,\mathrm{d}x_3\,,
\tag{25}
$$

where ρ^k is the mass density of the kth material layer, and parameters of damping are taken as

$$
(\widetilde{A}_{11}, \widetilde{B}_{11}, \widetilde{D}_{11}) = \sum_{k=1}^{n}\widetilde{Q}_{11}^k\int_{h_{k-1}}^{h_k}b(x_3)(1, x_3, x_3^2)\,\mathrm{d}x_3\,, \qquad \widetilde{A}_{55} = \sum_{k=1}^{n}\widetilde{Q}_{55}^k\int_{h_{k-1}}^{h_k}b(x_3)\,\mathrm{d}x_3\,.
\tag{26}
$$

As obvious from (13), each finite element is generally subjected to body forces and tractions. These loadings may be time dependent and therefore can be rewritten in the form

$$
\sum_{i=1,3}\left(\int_{V^e}\delta u_i\, X_i\,\mathrm{d}V + \int_{A_p^e}\delta u_i\, p_i\,\mathrm{d}A\right) = \delta\boldsymbol{q}_e^T(t)\boldsymbol{f}_e(t)\,,
\tag{27}
$$

where $\boldsymbol{f}_e(t)$ is the vector of element external loading.

Expressing the vector $\boldsymbol{q}_e$ using the corresponding localization matrix $\boldsymbol{J}_e$ for each element by the relation

$$
\boldsymbol{q}_e(t) = \boldsymbol{J}_e\,\boldsymbol{q}(t)
\tag{28}
$$

and substituting (20), (21) and (27) into (13), the solution of a problem by a finite element method leads to differential equations of the form

$$
\boldsymbol{M}\ddot{\boldsymbol{q}}(t) + \boldsymbol{B}\dot{\boldsymbol{q}}(t) + \boldsymbol{K}\boldsymbol{q}(t) = \boldsymbol{f}(t) \qquad \text{for} \qquad \delta\boldsymbol{q}^T(t) \neq \boldsymbol{0}\,,
\tag{29}
$$

where

$$
\boldsymbol{M} = \sum_e\boldsymbol{J}_e^T\boldsymbol{M}_e\boldsymbol{J}_e\,, \qquad \boldsymbol{B} = \sum_e\boldsymbol{J}_e^T\boldsymbol{B}_e\boldsymbol{J}_e\,, \qquad \boldsymbol{K} = \sum_e\boldsymbol{J}_e^T\boldsymbol{K}_e\boldsymbol{J}_e
\tag{30}
$$

are mass, damping and stiffness matrices, respectively, and

$$
\boldsymbol{f}(t) = \sum_e\boldsymbol{J}_e^T\boldsymbol{f}_e(t)
\tag{31}
$$

is time dependent vector of external loading. The vector $\boldsymbol{q}(t)$ represents generalized displacements in nodes that can be obtained by solving the system (29) with the help of some numerical integration method.

4. Analytical solution used for finite element verification

As mentioned above, the verification of derived finite element was performed using the analytical solution of a particular beam problem. The analytical solution of non-stationary vibration of a simply supported thin viscoelastic beam presented in [1] was used for this purpose. The geometry of this problem is depicted in Fig. 2. A thin beam of length $2l$ and with rectangular cross-section $b \times h$ is on its upper surface excited by a non-uniform tranverse external loading that is nonzero only on the region of length $2d$. The spatio-temporal function describing this loading was assumed in the form

$$q(x_1, t) = \sigma_a \, b \, \cos \frac{\pi(x_1 - l)}{2d} H(t) \qquad \text{for} \qquad x_1 \in \langle l - d, l + d \rangle, \tag{32}$$

where σ_a represents the excitation amplitude and $H(t)$ denotes the Heaviside function in time.
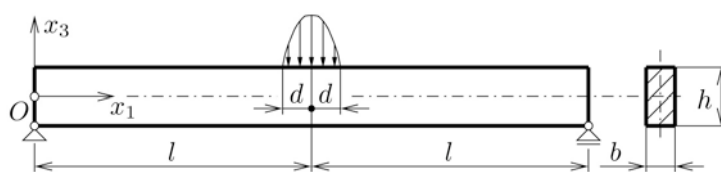

Fig. 2. Geometry of a simple supported beam with applied loading

Using the Timoshenko beam theory and solving the resulting system of two partial integro-differential motion equations by the method of integral transforms, the beam deflection function $w(x_1, t)$ and the beam slope function $\psi(x_1, t)$ can be expressed as infinite sums in the form [1]

$$w(x_1, t) = \sum_{n=1}^{\infty} C(n) \sin(\omega_n x_1) \mathcal{L}^{-1} \left\{ \frac{H_4(n, p)}{p H_6(n, p)} \right\},$$

$$\psi(x_1, t) = \sum_{n=1}^{\infty} C(n) \cos(\omega_n x_1) \mathcal{L}^{-1} \left\{ \frac{H_2(n, p)}{p H_6(n, p)} \right\}, \tag{33}$$

where the operator $\mathcal{L}^{-1}$ denotes the inverse Laplace transform and the real function $C(n)$ related to the applied loading is defined as

$$C(n) = 4 \, \sigma_a \, d \, b \, \frac{\cos\left(\frac{\pi n d}{2l}\right) \sin\left(\frac{\pi n}{2}\right)}{\pi l \left[1 - \left(\frac{nd}{l}\right)^2\right]}. \tag{34}$$

The complex functions $H_i(n, p)$ $(i = 2, 4, 6)$ in (33) are introduced by relations

$$H_2(n, p) = 12 \, \alpha \, \omega_n \, G^*(p), \qquad H_4(n, p) = h^2 \left(\rho \, p^2 + \omega_n{}^2 \, E^*(p)\right) + 12 \, \alpha \, G^*(p),$$

$$H_6(n, p) = b \, h \left[\left(\rho \, p^2 + \alpha \, \omega_n{}^2 \, G^*(p)\right) H_4(n, p) - \frac{1}{12} H_2(n, p)^2\right], \tag{35}$$

where $\omega_n = \frac{n\pi}{2l}$. Viscoelastic material properties of the beam are described by the complex moduli $E^*(p)$ a $G^*(p)$ which, in the case of generalized standard viscoelastic solid model with N parallel Maxwell elements, can be expressed as

$$E^*(p) = \sum_{k=0}^{N} E_{1_k} - \sum_{k=1}^{N} \frac{E_{1_k}^2}{\lambda_{1_k} p + E_{1_k}}, \qquad G^*(p) = \sum_{k=0}^{N} G_{31_k} - \sum_{k=1}^{N} \frac{G_{31_k}^2}{\eta_{31_k} p + G_{31_k}}. \tag{36}$$

The analytical solution for the Kelvin-Voight material model can be then simply obtained by the assumption $N = 1$ and $E_{1_1} \to \infty$.

5. Numerical results and discussion

In this section, the comparison of analytical and numerical results obtained by different integration methods and using two beam theories is given. Moreover, the verification of the analytical approach is performed with the help of FE solution using the software MSC.Marc. All computations were made for the problem depicted in Fig. 2 for the time interval $t \in \langle 0, 200 \rangle \, \mu$s under the assumption $\sigma_a = 1 \, \text{MPa}$ and $2 \, d = 4 \, \text{mm}$. Furthermore, the geometric dimensions were taken as $l = 50 \, \text{mm}$, $h = 10 \, \text{mm}$ and $b = 5 \, \text{mm}$. The value of the shear correction factor corresponds to arbitrary rectangular cross-section, i.e. $\alpha = 0.833$.

The parameters describing material behaviour of the beam studied were assumed as follows: $\rho = 2.1 \cdot 10^3 \, \text{kg} \, \text{m}^{-3}$, $E_1 = 39 \, \text{GPa}$, $G_{31} = 3.8 \, \text{GPa}$, $\lambda_1 = 35 \, \text{kPa s}$. Elastic and viscous Poisson's ratios were the same and equal to 0.28. It should be emphasized that the used material parameters do not correspond to a real material because it is nearly impossible to find values of all needed parameters for orthotropic material in literature. That is why some properties of unidirectional composite material E-glass/epoxy were used for the estimation of required parameters.

Points with coordinate $x_1 \in \{52, 60, 70\}$ mm, where the deflection and the slope of the beam were calculated, have been selected as points of interest. This choice allowed us to compare analytical and numerical solutions both in the vicinity of applied loading (the first point was identical to the boundary of loaded domain) and far from it. The computation of all presented problems have been done on a PC Pentium 4 with CPU 2.99 GHz and with RAM 3 GB.

5.1. Results given by MSC.Marc software

The numerical solution obtained using FE software MSC.Marc served for the verification of the analytical solution quality whereas the problem was solved as the problem of plane stress. Because the condition of symmetry were accepted, only the half of the beam geometry was modeled. The beam mesh consisted of 12500 regular four-node isoparametric elements with linear approximations. The basic element size 0.2×0.2 mm was chosen according to the work [1] and only the elements near the area of excitation were once refined to the half of their original size to reach better representation of applied loading. In addition to the zero axial displacement defined on the axis of symmetry, the boundary condition representing the beam support was prescribed in the first node at the bottom beam edge. Material properties of the beam were represented by the discrete viscoelastic model which is implemented in the used software.

The integration in time domain was performed by the Newmark method with a constant acceleration and with integration step $4 \cdot 10^{-8}$ s. This value was determined with respect to the maximum stable integration step of the explicit scheme of central differences [1]. This fact together with maximum time of interest led to very time-consuming computation which took about 4.7 hours.

As it is shown in Fig. 3, the comparison of the history plots of deflection w in points of interest between analytical (A.S. lines) and numerical (FEM lines) approach has been done. FEM results were investigated on the upper beam edge. It is obvious from Fig. 3(a) that both solution correspond each other quite well in all points studied. Moreover, the detailed view in Fig. 3(b) shows that some oscillations of the numerical solution occur. These phenomena are particularly clear for $x_1 = 52$ mm. The reason of these oscillations lies in the two-dimensionality of the FE numerical model. The obtained results show that the presented analytical solution may be employed for studying quality of derived finite element.
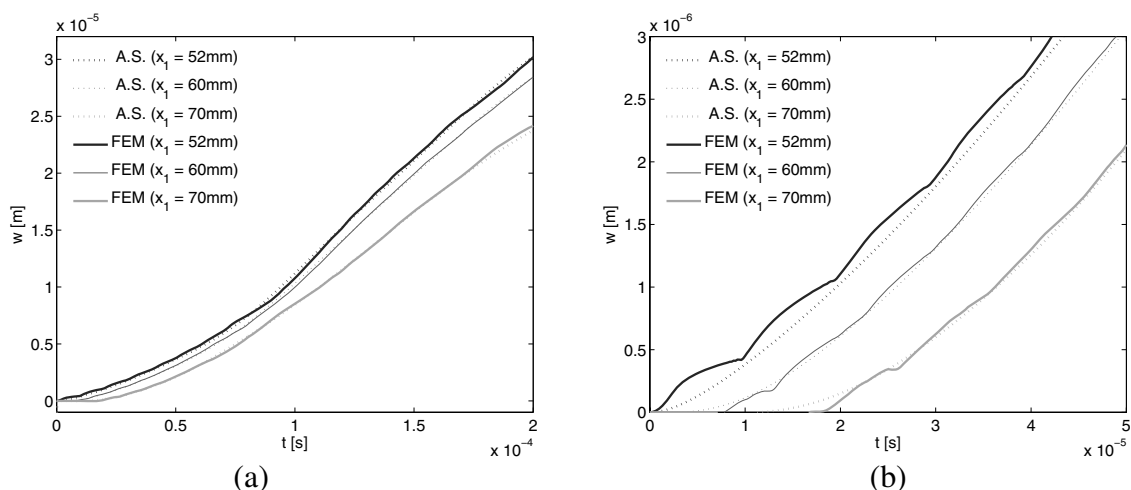
Fig. 3. History plot of beam deflection in points of interest (a) and detailed view (b). Analytical approach versus results given using software MSC.Marc

5.2. Results given by FE solution based on Euler-Bernoulli theory

In this part, numerical results computed using the finite elements developed based on the Euler-Bernoulli theory were compared with the analytical solution. For this purpose the FE model A built with 50 elements and FE model B built with 500 elements were presented. In both cases, finite elements were taken with the constant length along longitudinal beam axis. Euler-Bernoulli beam elements needed in these analyses can be simply obtained by omitting the vector ϕ_5 in (11). Therefore, the derived element in this part was utilized with some simplifications. Only essential boundary conditions, i.e. zero displacements at the end nodes of mesh according to Fig. 2, were applied in cases A and B.

Central difference method with integration step $1.25 \cdot 10^{-7}$ s (problem A) and Newmark method with a constant acceleration and with integration step $1 \cdot 10^{-7}$ s (problem B) were used for numerical integration of the system (29). Time steps were chosen with respect to the elements length and to the phase velocity of longitudinal wave in a thin rod. That is why the computation times of A and B problems were 0.8 s and 56 s, respectively, when the whole time interval $t \in \langle 0, 200 \rangle$ μs were taken into account.

It is observed from Fig. 4 given for the beam deflection (a) and the slope of beam (b) that correspondence between analytical and numerical results is rather bad. We can find cumulative difference in the beam deflection at all points of interest with increasing time. The curves describing the beam slope have even different form. Consequently, FE model contained 500 elements and solved with the help of central difference method was made but results were similar to them in the case B.

5.3. Results given by FE solution based on Timoshenko theory

In what follows, numerical tests using the Timoshenko beam theory are performed to confirm the quality of the finite element derived. Therefore, deformations of simply supported beam for variants 1 to 5 shown in Table 1 were studied. As can be seen for individual models in this table, meshes of solved problems consisted of 50 or 500 elements of equal lengths. Further, boundary conditions and numerical integration methods were used, as well as in cases of finite element models based on the Euler-Bernoulli theory.

It is clear from Table 1 that beam deformations obtained by FEM (in time $t = 200\,\mu$s) are slightly different from their exact values (errors are less than $0.2\,\%$). Similarly, good agreements
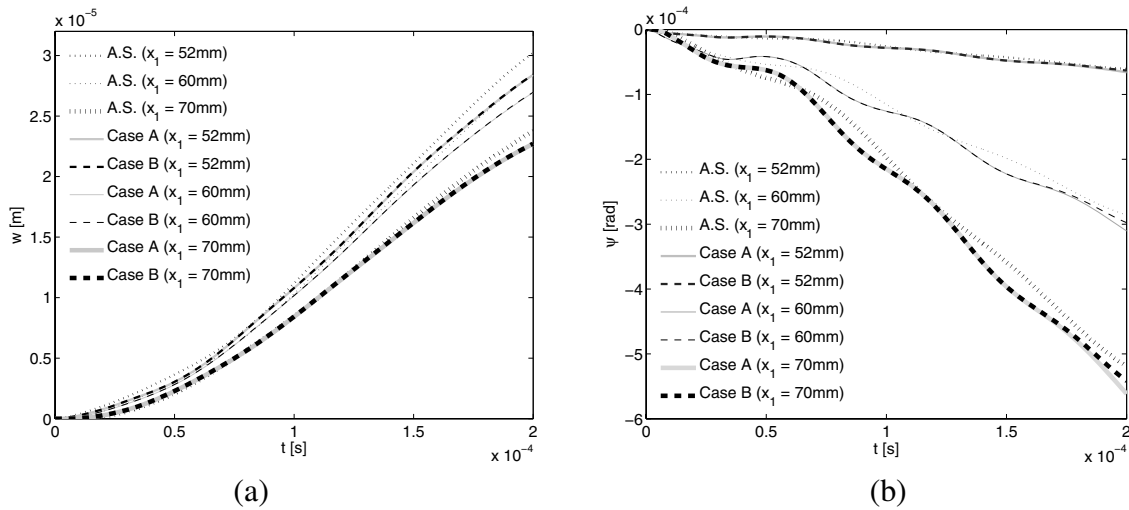
Fig. 4. History plot of beam deflection (a) and slope of beam (b) in points of interest. Analytical approach versus FE solution based on Euler-Bernoulli theory

Table 1. Comparison of numerical and analytical results in time $200\,\mu$s

Model m	Method	Elem.	Integration step [s]	CPU time [s]	Error [%] ($T = 200\,\mu$s)					
					w			ψ		
					x_1 [mm]					
					52	60	70	52	60	70
1	Cent. diff.	500	2.50e$-$8	216	0.013	0.013	0.005	0.050	0.019	0.011
2	Newmark	500	1.00e$-$7	54	0.001	0.001	$-$0.008	0.040	0.008	$-$0.001
3	Cent. diff.	50	2.50e$-$7	0.58	0.194	0.185	0.167	0.110	0.079	0.069
4	Newmark	50	1.00e$-$6	0.23	0.074	0.063	0.043	0.005	$-$0.031	$-$0.047
5	Newmark	50	2.50e$-$7	0.61	0.074	0.063	0.042	0.010	$-$0.026	$-$0.045

in absolute values of deformations are found in all points of investigated time interval. In order to make the mutual comparison of results accuracy over all cases ($m = 1, \ldots, 5$), following parameters have been defined:

$$w^*(x_1, t, T)\big|_r^m = \frac{w_m(x_1, t) - w_{\text{A.S.}}(x_1, t)}{w_r(x_1, T) - w_{\text{A.S.}}(x_1, T)},$$

$$\psi^*(x_1, t, T)\big|_r^m = \frac{\psi_m(x_1, t) - \psi_{\text{A.S.}}(x_1, t)}{\psi_r(x_1, T) - \psi_{\text{A.S.}}(x_1, T)}, \tag{37}$$

where $w_m(x_1, t)$ and $w_{\text{A.S.}}(x_1, t)$ is beam deflection calculated from mth problem and analytical solution, respectively. In the analogous way, the notation of beam slope $\psi_m(x_1, t)$ and $\psi_{\text{A.S.}}(x_1, t)$ is employed. It is shown in Table 1 that the minimum difference were found for model $m = 2$. Consequently, the parameter $r = 2$ were taken for the calculation of $w^*|_r^m$ and $\psi^*|_r^m$ in (37). Fig. 5 shows history plots of these parameters in selected points of interest within the time interval $\langle 0, T \rangle$ where $T = 200\,\mu$s. It is obvious from this figure that both solutions with a fine-mesh discretization ($m = 1, 2$) give very good results over the whole time interval but the best results are explicitly found for $m = 2$. Furthermore, comparing results of all studied variants (mainly the deflections in Fig. 5(a) and Fig. 5(b)) it can be said that the better accuracy with
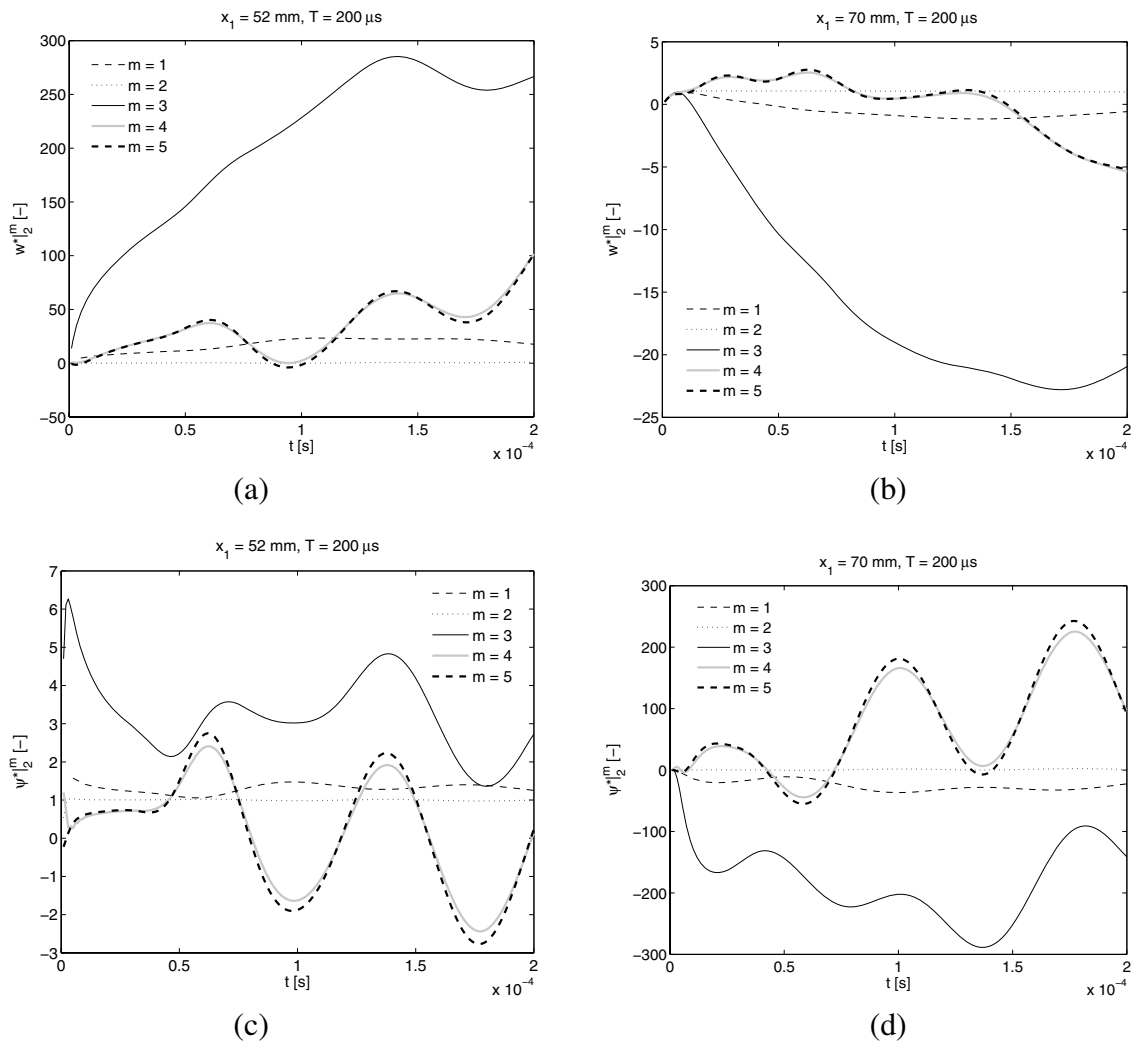
Fig. 5. History plot of parameters $w^*|_r^m$ and $\psi|_r^m$ for $r = 2$ and $T = 200\,\mu$s in some points of interest. FE solution based on Timoshenko theory

respect to results of the model 2 can be achieved by the use of the Newmark integration method. The history plots for point of interest $x_1 = 60$ mm were analysed as well but changing curves characters were similar to the case $x_1 = 70$ mm. Therefore these curves are not presented in this work.

6. Conclusion

The finite beam element for solving orthotropic viscoelastic problems was derived based on the Timoshenko theory using the principle of virtual work. The discrete Kelvin-Voight model was used for the description of its material behaviour. The validation of this element was made with the help of analytical solution and of the FE system MSC.Marc on the problem of simply supported beam subjected to a transverse non-stationary loading. Concretely, the time distribution of the beam deflection and the slope of the beam were compared in time interval 0 to $200\,\mu$s and in three specific points ($x_1 \in \{52, 60, 70\}$ mm), one of which was situated in the vicinity of the loading applied. The beam deformations were calculated using the derived element, whereas the Euler-Bernoulli theory and the Timoshenko theory were taken into account. The meshes of

numerical models consisted of 50 or 500 elements and the Newmark method or the method of central differences were used for the integration in time domain. Based on the computations performed, one can say that the developed finite element gives very accurate results and its usage is connected with significantly lower CPU-time than in the case of analytical approach. With respect to this fact, this element seems to be suitable for the effective solution of inverse problems.

Acknowledgements

References

[1] Adámek, V., Valeš, F., A viscoelastic orthotropic beam subjected to general transverse loading, Applied and Computational Mechanics 2 (2) (2008) 215–226.

[2] Altenbach, H., Altenbach, J., Kissing, W., Mechanics of composite structural elements, Springer, Berlin, 2004.

[3] Davis, R., Henshell, R. D., Wanburton, G. B., A Timoshenko beam element. Journal of Sound and Vibration (22) (1972) 475–487.

[4] Graff, K. F., Wave motion in elastic solids, Clarendon Press, Oxford, 1975.

[5] Heyliger, P. R., Reddy, J. N., A high order beam finite element for bending and vibration problems. Journal of Sound and Vibration (126) (1988) 309–326.

[6] Chandrashekhara, K., Krishnamurthy, K., Roy, S., Free vibration of composite beams including rotary inertia and shear deformation. Composite Structures (14) (1990) 269–279.

[7] Liu, G. R., Xi, Z. C., Elastic waves in anisotropic laminates, CRC Press, Boca Raton, 2002.

[8] Subramanian, P., Dynamic analysis of laminated composite beams using higher order theories and finite elements. Composite Structures (73) (2006) 342–353.

[9] Stephan, N. G., Levinson, M. A., A second-order beam theory. Journal of Sound and Vibration (67) (1979) 293–305.

[10] Thomas, J., Abbas, B. A. H., Finite element model for dynamic analysis of Timoshenko beams. Journal of Sound and Vibration (41) (1975) 291–299.

[11] Zajíček, M., Linear elastic analysis of thin laminated beams with uniform and symmetric cross-section, Applied and Computational Mechanics 2 (2) (2008) 397–408.

[12] Zienkiewicz, O. C., Taylor, R. L., Finite element method for solid and structural mechanics, Elsevier, Oxford, 6th edition, 2005.